

Grain Size Distributions and Photo-Electric Heating in Ionized Regions

P.A.M. van Hoof¹, J.C. Weingartner², P.G. Martin², K. Volk³, G.J. Ferland⁴

¹Queen's University Belfast, APS Division, Belfast, BT7 1NN, Northern Ireland

²CITA, 60 St. George Street, Toronto, ON M5S 3H8, Canada

³University of Calgary, 2500 University Dr. NW, Calgary, AB T2N 1N4, Canada

⁴University of Kentucky, 177 CP Building, Lexington, KY 40506, USA

1. Introduction

This poster focuses on the grain model in Cloudy, which has undergone a major upgrade in the last couple of years. The first grain model was introduced to Cloudy in 1990 to facilitate more accurate modeling of the Orion nebula (for a detailed description see Baldwin et al., 1991, ApJ 374, 580). In subsequent years, this model has undergone some revisions and extensions, but remained largely the same. Recently, our knowledge of grains has been greatly advanced by the results from the ISO mission. In view of these rapid developments we have undertaken a major upgrade of the grain model in Cloudy. The two main aims were to make the code more flexible and versatile, and to make the modeling results more realistic.

At this meeting we present new results obtained with this code which underline the strong effect of photo-electric heating by grains in photo-ionized regions. More in particular we will study the effect that the distribution of grain sizes has on the magnitude of the effect. We will show that this effect is nothing short of dramatic, making the grain size distribution an important parameter in modeling of photo-ionized regions such as H II regions and planetary nebulae. Only few studies of grain size distributions exist, and they mainly concentrate on the diffuse interstellar medium (ISM) in order to explain extinction curves. Further study of grain size distributions will be needed in order to enable more accurate modeling of photo-ionized regions. This is especially the case for planetary nebulae since it is not clear whether ISM size distributions are valid for these objects.

This poster will start with a general description of the new features in the Cloudy grain code in Sects. 2.1 through 2.3. The model calculations of dusty photo-ionized regions are discussed in Sect. 3.

2.1 Resolving the grain size distribution

In the original model, grain opacities for a handful of grain species were hard-wired in the code. Furthermore, all physical properties of the grains (such as opacity, equilibrium temperature, charge, photo-electric heating, etc.) were integrated/averaged over the entire size distribution. This is usually a bad approximation because most grain properties depend strongly (and more importantly non-linearly) on grain size. A prime example is the grain opacity (shown in Figure 1). When the first grain model was introduced in Cloudy these approximations were necessary due to computational limitations. However, thanks to Moore's law this is no longer the case. So, to improve the model, we have implemented the following changes:

- We have included a Mie code for spherical particles in Cloudy. The necessary optical constants needed to run the code are read from a separate file. This allows greater freedom in the choice of grain materials. Files with optical constants for a range of materials are included in the Cloudy distribution. However, users can also supply their own optical constants for a completely different grain type.
- A mixing law has been introduced to the code. This allows the user to define grains which are mixtures of different materials. Cloudy will then calculate the appropriate opacities by combining the optical constants of these grain types.
- The absorption and scattering opacities can be calculated for completely arbitrary grain size distributions (including single-sized grains). The size distribution can either be defined using an analytic expression with tunable parameters, or by supplying a table, giving the user even more freedom.
- The size distribution can be resolved in many small bins (the user can choose how many), and all physical quantities are calculated for each bin separately. This allows non-equilibrium heating to be treated correctly for the smallest grains in the size distribution (see § 2.2), and more realistic grain emission spectra to be calculated. It will also improve the prediction for the magnitude of the photo-electric effect which also depends strongly on grain size.

2.2 Non-equilibrium heating of small grains

It is well known that in conditions where the cooling time of the grain is shorter than or comparable to the average time between two significant heating events, a non-equilibrium treatment of the grain temperature is necessary (Guhathakurta & Draine 1989, ApJ 345, 230, and references therein). This effect is important for grains smaller than roughly 200 Å (most notably for polycyclic aromatic hydrocarbons or PAH's), and/or in regions where the photon density is very low (e.g., the ISM). A code implementing non-equilibrium treatment of PAH's was already included in a revision to the old grain model. This code has been extensively rewritten for the new grain model. It now works automatically and efficiently with all grain types and sizes, under all conditions.

To highlight the importance of non-equilibrium heating, we show in Figure 2 the emitted spectrum from a 50 Å silicate grain in typical diffuse ISM conditions using the old and new grain model.

2.3 Changes to the grain physics

We have modified certain aspects of the grain physics following the discussion in Weingartner & Draine (2001, ApJS 134, 263). Below we highlight certain aspects of these changes.

- We now include the bandgap between valence and conduction band in our potential well model for silicates. Tunneling effects are also included using an analytic fit to calculations using the WKB approximation.
- The treatment of the photo-electric effect has been improved.
- The treatment of electron sticking probabilities has been updated. This has an important impact on the photo-electric heating rate of the gas (especially when very small grains are present). The sticking probability has a strong effect because under most circumstances photo-electric heating scales linearly with the sticking probability.
Caution: Since the sticking probability is very poorly known (only to factors of a few or worse), the predicted photo-electric heating rate is just as uncertain and should be viewed with caution.
- Our treatment deviates somewhat from Weingartner & Draine (1999) in that we use the hybrid grain charge model (van Hoof et al., 2001, ASP Conference Series, Vol. 247, p. 363), instead of a fully resolved non-equilibrium charge distribution. We have shown that the hybrid grain charge model is sufficiently accurate for all realistic astronomical applications.

3 Photo-electric heating and grain size distributions

It is well known that photo-electric heating by grains in a photo-ionized region has an important effect on the emitted spectrum (e.g., Volk, 2001, ASP Conference Series, Vol. 247, p. 379; Dopita & Sutherland, 2000, ApJ 539, 742). It is however not well known that the size distribution of the grains plays a very important role in determining the magnitude of this effect. In order to test this, we have constructed a set of models with Cloudy 96 beta 5 based on the standard Paris H II and PN models (Péquignot, 1986, “Model Nebulae”, Publications de l’Observatoire de Paris). The base models contain no dust, and will be used as a point of reference. We constructed 6 models out of each base model by simply adding a dust component. We stress that in all six models the chemical composition and the dust-to-gas mass ratio of the dust is the same, and the only difference is the size distribution. Two models were using single sized grains of 1.0 and 0.1 μm , while the other 4 were using more or less realistic size distributions taken from the literature. We also point out that the models are ionization bounded, so the outer radius varies, depending on the total opacity of the grains (which also depends strongly on the size distribution, see Figure 1). For the Paris H II model we added a mixture of graphite and silicates, while for the Paris PN models we made separate models for graphite and silicates since these grain types are not expected to co-exist. In Figures 3, 4, and 5 we show the results of these calculation. In the top-left panel we show the strength of selected infrared fine-structure lines. These are expected to be mostly insensitive to electron temperature and therefore show the difference in the overall ionization structure. In the top-right panel we show optical/UV forbidden lines of the same species, clearly showing that the enhancement for these lines is usually much stronger, especially for highly excited lines which are only populated in the inner regions of the nebula. This clearly shows the excess collisional excitation caused by the photo-electric effect. In the bottom panel of each plot this is further illustrated by showing the electron temperature at the inner edge, as well as averaged over the ionized region, and the fraction of the total gas heating that is due to the photo-electric effect.

All these plots clearly illustrate that the size distribution alone has a dramatic effect on the emitted spectrum, and is therefore an important parameter in the modeling of spectra from H II regions and PN. More research will be needed to get a better understanding of this parameter. This is especially the case for planetary nebulae since it is not clear whether ISM size distributions are valid for these objects.

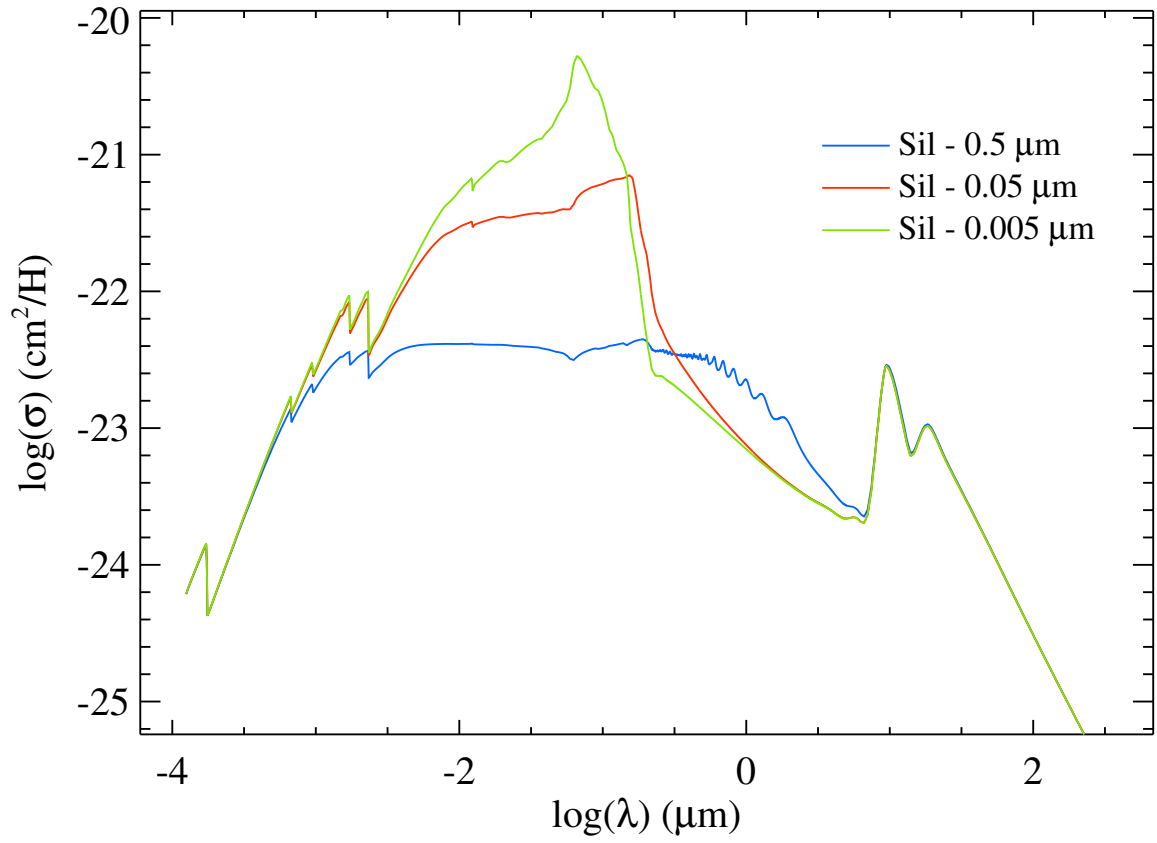


Fig. 1 – The absorption cross section for astronomical silicate for three single sized grains. The dust-to-gas ratio is the same for all three species and the cross sections are normalized per hydrogen nucleus in the plasma.

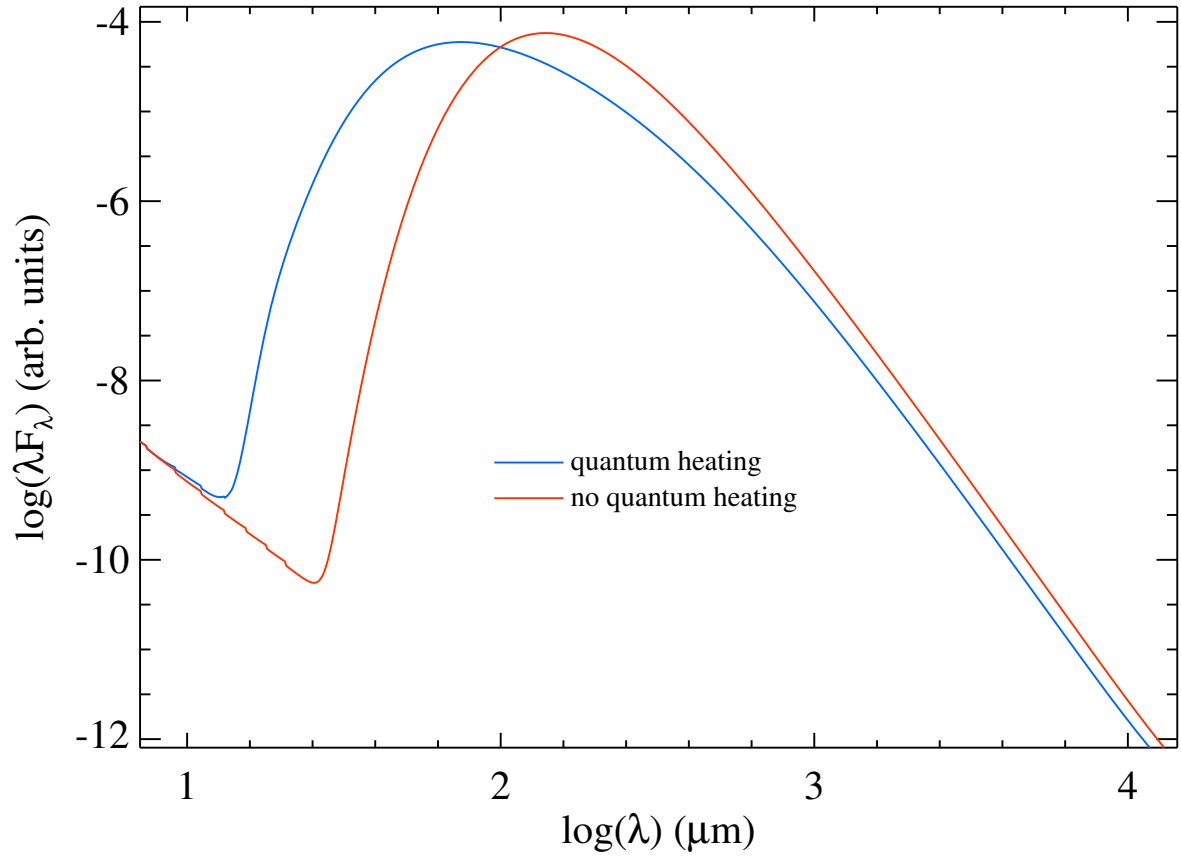
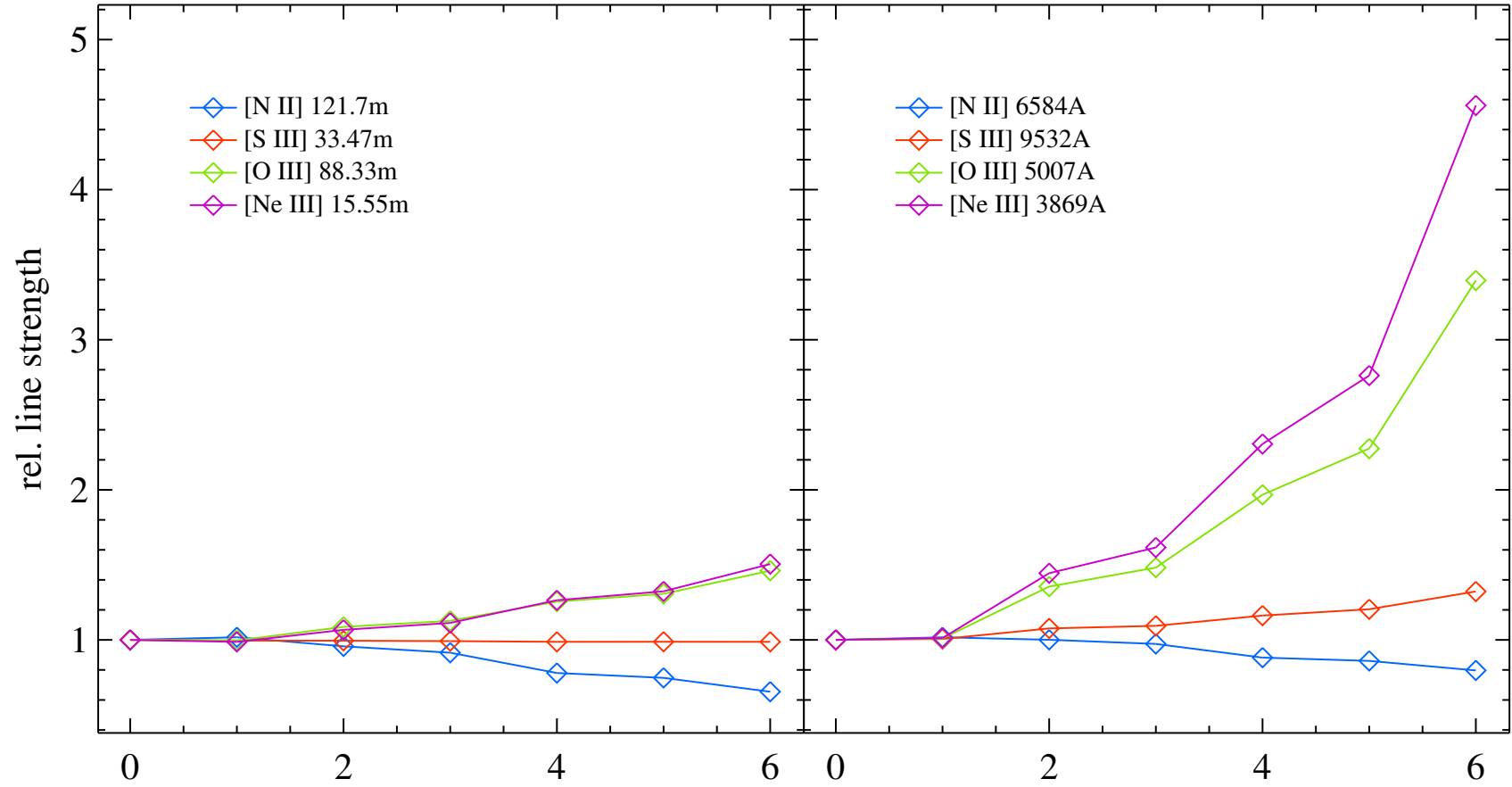


Fig. 2 – Model predictions for the emission from a 50 Å silicate grain in typical diffuse ISM conditions. The red line shows the model assuming that all grains have the same equilibrium temperature (i.e., non-equilibrium heating effects are turned off). The blue line shows the model including non-equilibrium effects. The model is for a hydrogen column density of 10^{20} cm^{-2} , the continuum visible around $10 \mu\text{m}$ is the interstellar radiation field from nearby stars.



model 0: no grains
 model 1: single size 1.0 μ m
 model 2: single size 0.1 μ m
 model 3: Mathis, Rumpl & Nordsieck, 1977, ApJ 217, 425, truncated, $R_V=5.5$
 model 4: Kim, Martin & Hendry, 1994, ApJ 422, 164, $R_V=5.3$
 model 5: Weingartner & Draine, 2001, ApJ 548, 296, model A0, $R_V=5.5$
 model 6: Weingartner & Draine, 2001, ApJ 548, 296, model A3, $R_V=5.5$

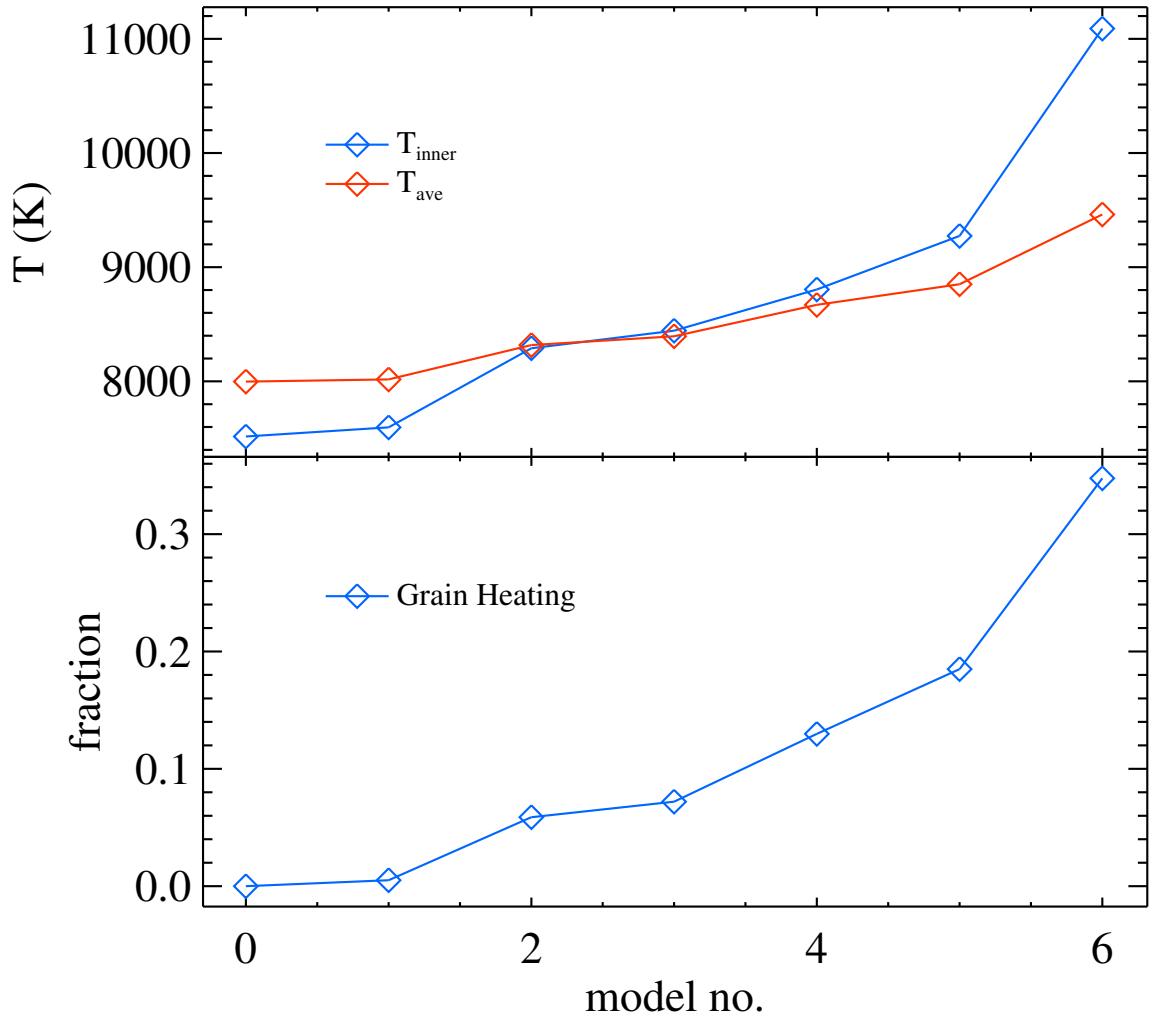
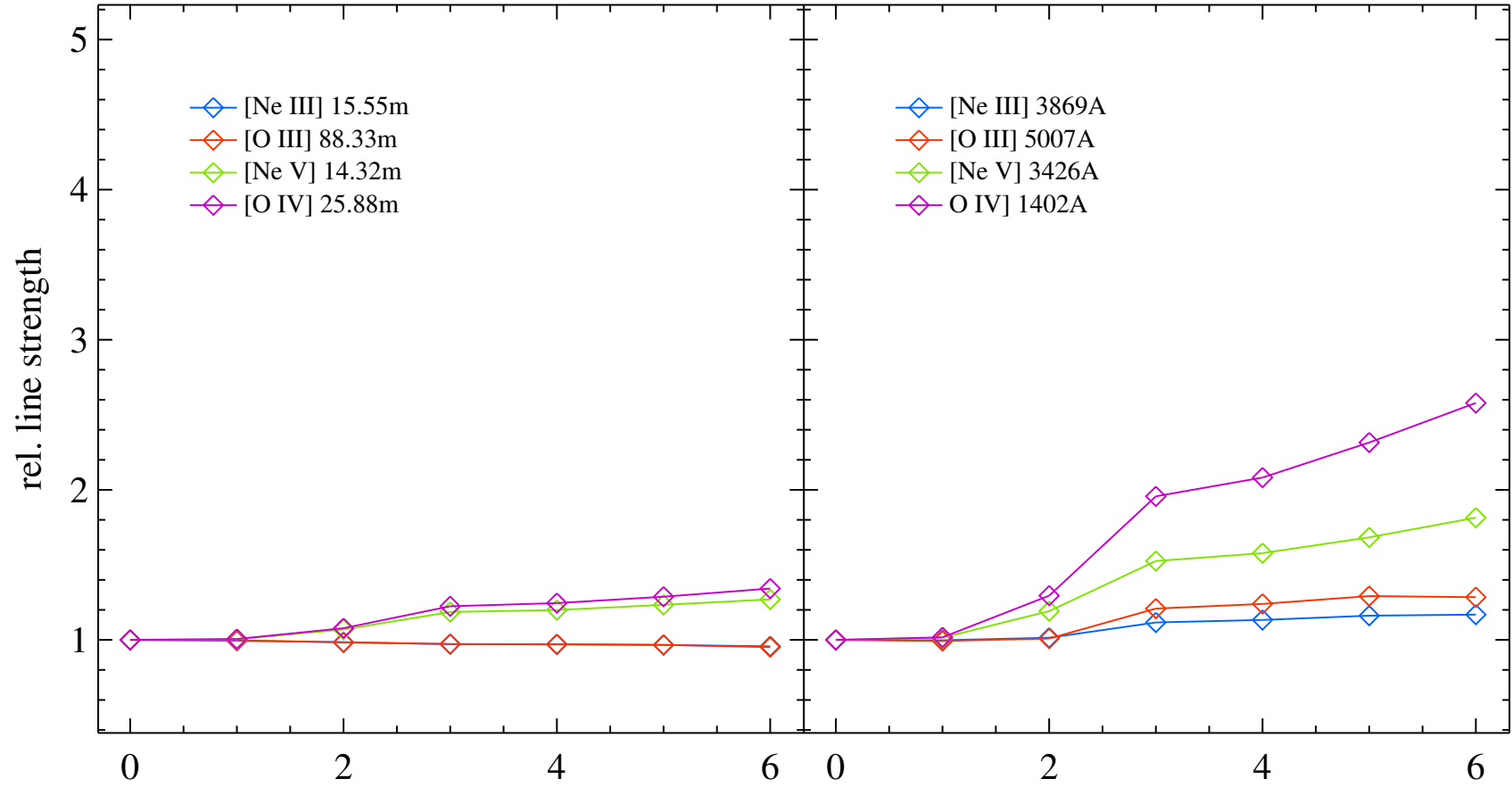


Fig. 3 – Paris H II models. In the top left panel we show the relative line strengths for selected infrared fine-structure lines. These are expected to be mostly insensitive to electron temperature and therefore show the difference in the overall ionization structure. The line strengths are normalized to the line strength in the dust-free model. In the top-right panel we show optical/UV forbidden lines of the same species. In the bottom panels we show the electron temperature at the inner edge, as well as averaged over the ionized region, and the fraction of the total gas heating that is due to the photo-electric effect. See Sect. 3 for further details.



model 0: no grains
 model 1: single size $1.0\mu\text{m}$
 model 2: single size $0.1\mu\text{m}$
 model 3: Mathis, Rumpl & Nordsieck, 1977, ApJ 217, 425, $R_V=3.1$
 model 4: Weingartner & Draine, 2001, ApJ 548, 296, model A0, $R_V=3.1$
 model 5: Kim, Martin & Hendry, 1994, ApJ 422, 164, $R_V=3.1$
 model 6: Weingartner & Draine, 2001, ApJ 548, 296, model A6, $R_V=3.1$

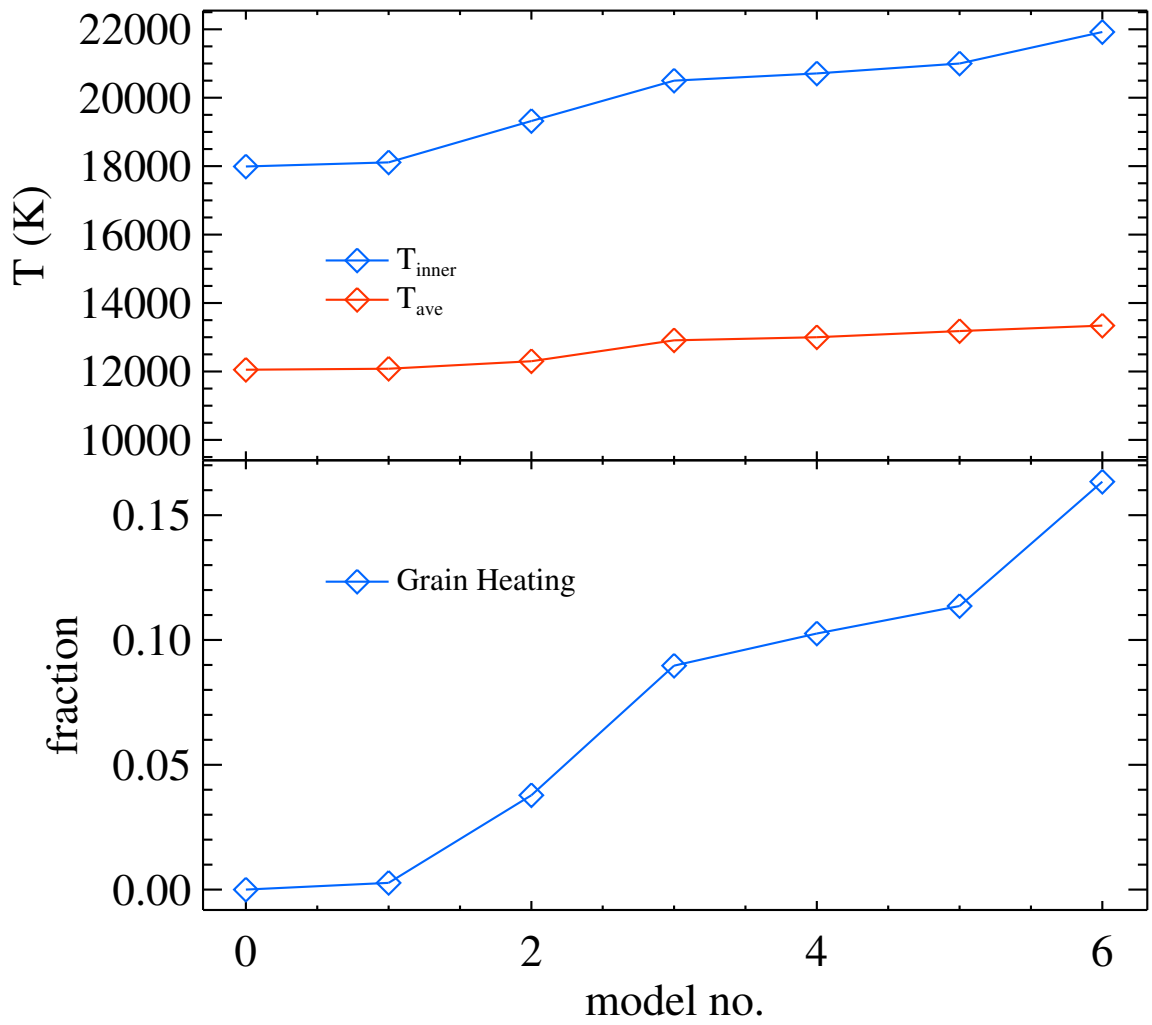
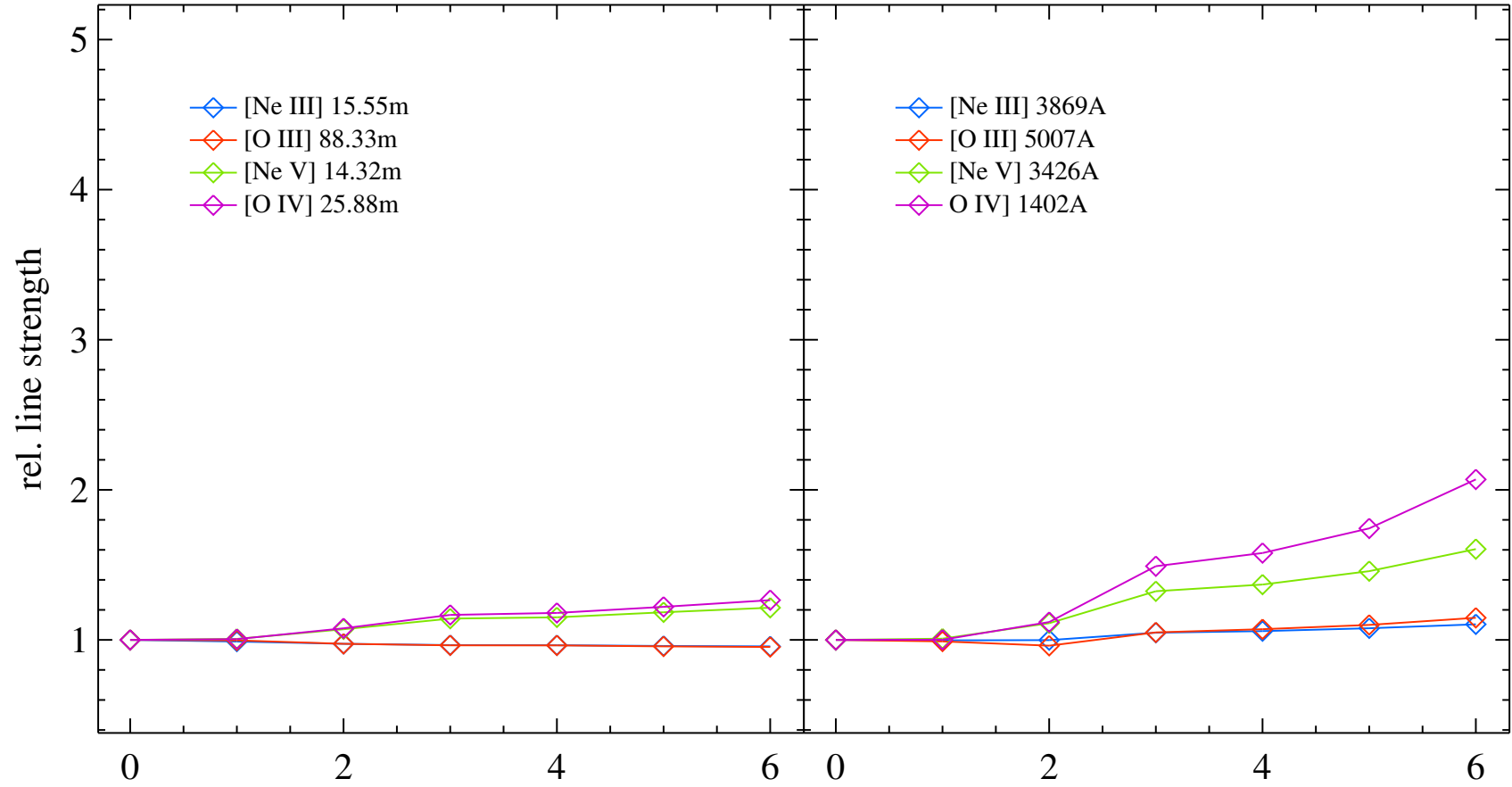


Fig. 4 – Same as Fig. 3, but for the Paris PN models with graphite only.



model 0: no grains
 model 1: single size $1.0\mu\text{m}$
 model 2: single size $0.1\mu\text{m}$
 model 3: Weingartner & Draine, 2001, ApJ 548, 296, model A0, $R_V=3.1$
 model 4: Weingartner & Draine, 2001, ApJ 548, 296, model A6, $R_V=3.1$
 model 5: Mathis, Rumpl & Nordsieck, 1977, ApJ 217, 425, $R_V=3.1$
 model 6: Kim, Martin & Hendry, 1994, ApJ 422, 164, $R_V=3.1$

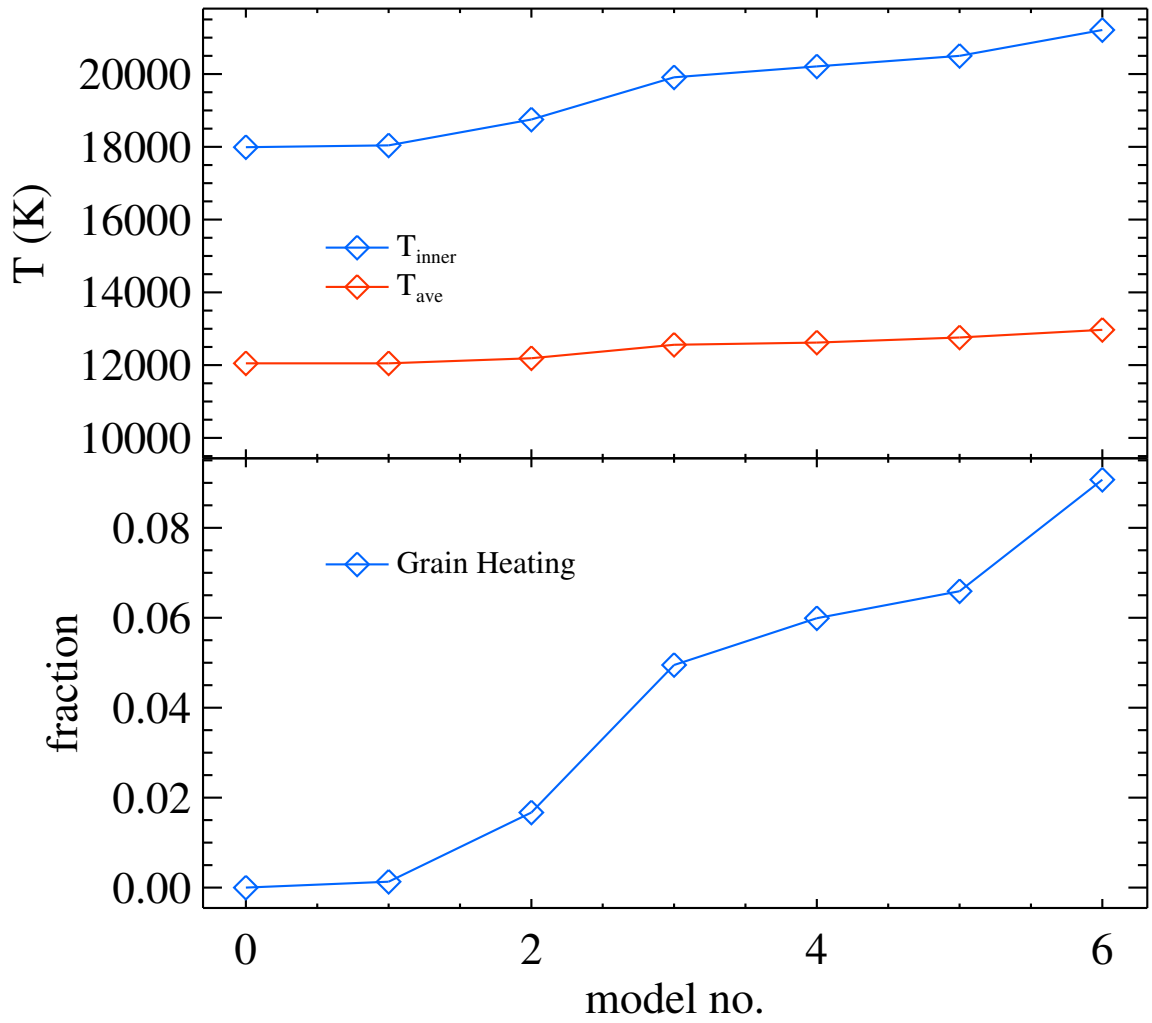


Fig. 5 – Same as Fig. 3, but for the Paris PN models with silicate only.